Pull-out Experiments of Flip-Type End Anchors Buried or Pushed in Model Ground of Dry Sand

Shota YOSHIDA
Civil engineer, Daisho Corporation, Nagahama, Shiga, Japan
Masanori KANNO
Engineer, Hokuriku Regional Development Bureau, Ministry of Land, Infrastructure, Transport and Tourism, Japan
Tatsunori MATSUMOTO
Professor, Graduate School of Kanazawa University, Kanazawa, Japan
Email: matsumoto@se.kanazawa-u.ac.jp
Shinya SHIMONO
Technician, Kanazawa University, Kanazawa, Japan
Takayoshi YOSHIDA
Civil engineer, Daisho Corporation, Nagahama, Shiga, Japan
Shun-ichi KOBAYASHI
Associate Professor, Graduate School of Kanazawa University, Kanazawa, Japan

ABSTRACT

End-resistance type earth anchors are often employed to reinforce slopes or to ensure slope stability. Hulk Earth anchor developed by Anchoring Rope and Rigging Pty Ltd (AR+R) in Australia is one of flip-type end earth anchors (hereafter, flip anchor). The flip anchor is installed in the ground by driving or press-in. When the flip anchor is installed in the ground, the end plate is closed to facilitate the penetration process. When pull-out force is applied to the anchor through pulling rod or wire, it is expected that the end plate is opened with increasing the pull-out displacement to enhance the pull-out resistance. At present, pull-out resistance mechanism of the flip anchors has not been fully understood. Hence, in this research, fundamental push-in and pull-out experiments were carried out to investigate performance of the flip anchors in dry sand model ground. Furthermore, push-up experiments of a trap door in a dry sand model ground simulating an anchor were carried out to investigate the mechanism of the resistance of the anchor in plane strain condition. An image analysis of the ground deformation was conducted in this series of the experiments. A simple model of the ground failure was used to obtain theoretical values of the pull-out resistance of the anchor.

Key words: *End-anchor, Pull-out resistance, Dry sand, Jack-in installation, Buried installation*

1. Introduction

1. 1. Background

Heavy rains and/or strong winds often cause slope failures, and collapses of towers and vinyl houses (plastic greenhouses).

One of emergency and prompt counter measures against these damages is the use of end-anchors that can be installed in the ground by press-in or driving. A flip type end anchor, called Hulk earth anchor, has been developed in Australia (Anchoring Rope and Rigging Pty Ltd, 2018).

1. 2. Flip-type earth anchor

The flip anchor is known as a kind of end-anchors which is used to reinforce slopes or support towers or pipe lines. The anchor is driven or pressed into the ground by using a driving rod with its head closed (**Fig. 1a**). After the completion of the anchor installation, the

driving rod is removed and the anchor is pulled with pulling rod or pulling wire. It is expected that the anchor head will be opened during the pulling process, as shown in **Fig. 1b**, to enhance the pull-out resistance.

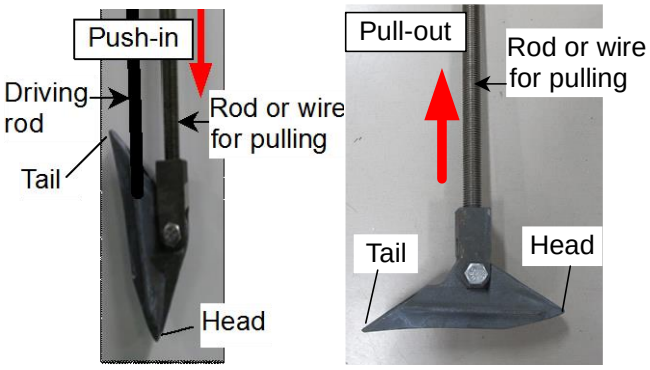

(a) Installation process (b) Pull-out process

Fig. 1 Example of flip anchor

1.3. Objectives and contents of the research

A design method for the flip type anchor has not fully been established. Hence, an objective in this research is to investigate fundamental pull-out resistance mechanisms of the anchor through a series of push-in and pull-out experiments, and pull-out experiments of the anchors in dry sand model ground.

Furthermore, push-up experiments of a trap door simulating an anchor were carried out, in order to investigate mechanisms of the pull-out resistance of anchors in more simplified experimental conditions (plane strain conditions). A theoretical consideration is made for the experimental results.

2. Outline of experiments

Two types of experiments were carried out in this paper.

Anchors were pressed into the model ground to different depths, and then they were pulled out. This type of experiment is called "press-in and pull-out experiment (PI & PO test)". In another type of experiment, anchors were embedded in the model ground during its preparation, and a pull-out experiment (PO test) was carried out. The same model ground and anchors were used in these experiments.

2.1. Model ground

The model ground was prepared in the rigid rectangular soil box with a height of 530 mm, a length of 800 mm and a width of 500 mm (**Fig. 2**). Dry silica sand #6 was used for the model ground. Physical properties of the sand are listed in **Table 1**.

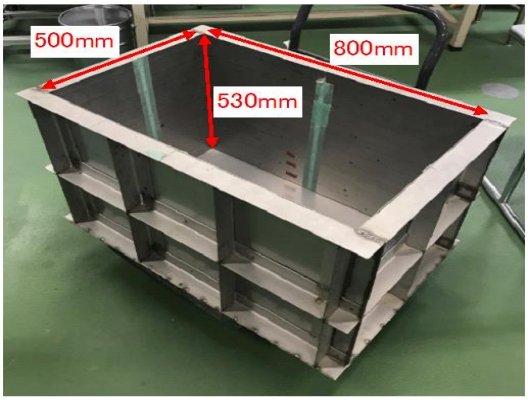

Fig. 2 Soil box

Table 1. Physical properties of dry silica #6

Density of soil particle, ρ_s (g/cm^3)	2.67
Maximum dry density, ρ_{dmax} (g/cm^3)	1.604
Minimum dry density, ρ_{dmin} (g/cm^3)	1.268
Maximum void ratio, e_{max}	1.089
Minimum void ratio, e_{min}	0.652
Cohesion at peak strength, c_p' (kN/m^2)	10.3
Int. friction angle at peak strength, ϕ_p' (deg)	38.6
Cohesion at residual strength, c_r' (kN/m^2)	4.6
Int. friction angle at residual strength, ϕ_r' (deg)	34.8

The model ground was prepared with 10 soil layers of 50 mm thick and one layer of 30 mm thick. The sand was put into the soil box for each layer, and the sand layer was compacted to get a designated density (relative density D_r = 82%, dry density ρ_d = 1.533 g/cm^3). This procedure was repeated to complete the model ground of 530 mm high.

2.2. Anchors used

Three types of flip anchors were used in the experiments. The dimensions of the anchors are indicated in **Fig. 3**. They are named S-, M- and L-anchors, according to the project area, *A*.

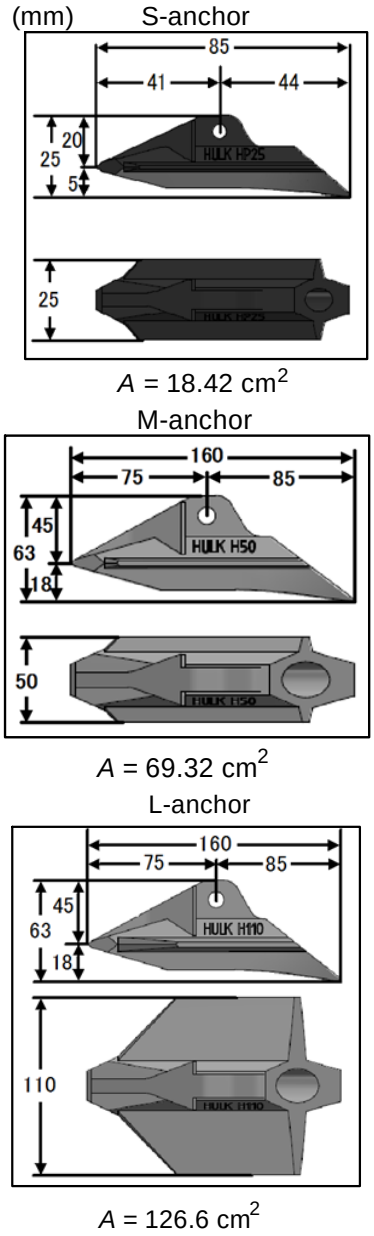

Fig. 3 Geometrical properties of anchors

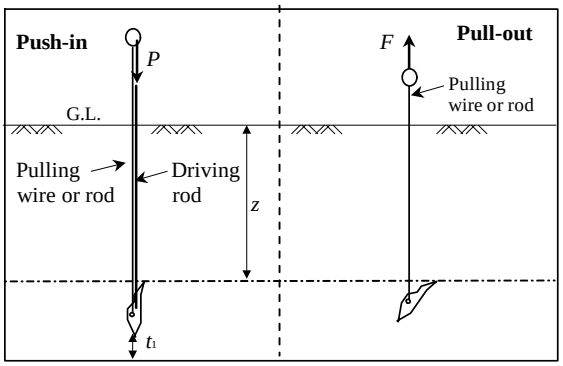

Fig. 4 Illustration of push-in and pull-out experiment

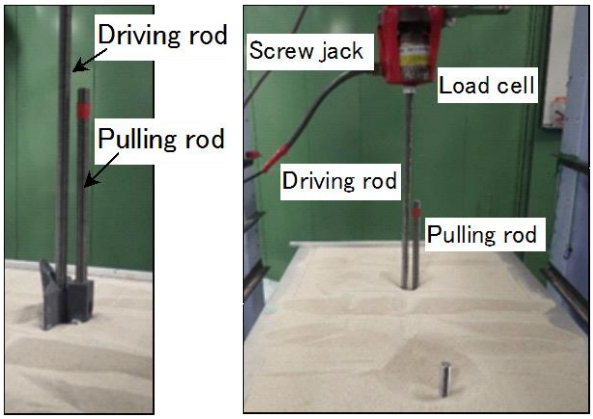

Fig. 5 Photos of press-in process of an anchor

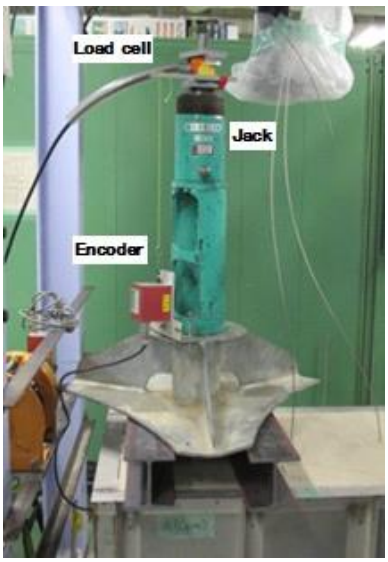

Fig. 6 Equipment for pulling out anchors

3. Push-in and pull-out experiments

3.1. Experimental procedure

In PI & PO test, first, the anchor was pressed (pushed) into the model ground with its head closed (**Figs. 4 and 5**) to a designated depth by means of a screw jack set on the driving rod. A load cell was placed between the screw jack and the head of the driving rod to measure the push-in force. Displacement of the anchor was measured using an encoder attached to the top of the driving rod.

After the anchor was penetrated to a designated depth, pull-out test was carried out subsequently, using the equipment shown in **Fig. 6.** A pair of H-shaped steel bars was placed on the soil box. And, a bearing stand having a centre-hole, a centre-hole type oil jack and a centre-hole type load cell were set on the H-shaped steel bars. The pulling rod was passed through the centre-holes, and its top was fixed on the top of the load cell with a reaction plate, so that compression force of the oil jack

gives tension force to the anchor. In this loading system, reaction force of the anchor is not transmitted to the ground surface.

A total of 9 cases of push-in and pull-out tests were carried out using three types of the anchors with different penetration depths, *z*.

3.3. Experimental results

Fig.7 shows the relationships between the push-in force, *P*, and the downward displacement, *w*, for L-anchor. Note that *w* in the figure is the depth of the head of the anchor. This is larger than the embedded depth of the anchor, *z*, by 160 mm (see **Fig. 3**). The three curves are almost identical, showing a repeatability of the model ground.

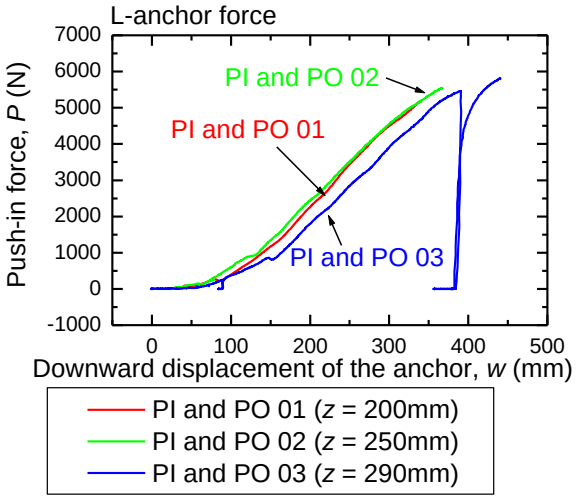

Fig. 7 Results of push-in tests of L-anchor

Fig. 8 shows the relationships between the maximum push-in force, P_{max}, and the embedment depth, *z*, of the S-, M- and L-anchors. For all the anchors, experiments with an embedment depth of 250 mm were conducted.

Hence, the relationships between the pull-out force, *F*, and the upward displacement, *w*, of all the anchors are compared in **Fig. 9**. The peak values of *F* were caused by relatively small displacement less than 10 mm in M- and L-anchors, although the peak F of S-anchor was caused by a larger displacement of 50 mm. After the peak forces, sharp softening behaviours were observed in all the anchors.

Fig. 10 shows the relationships between the maximum pull-out force, F_{max}, and the embedment depth, *z*, of the anchors.

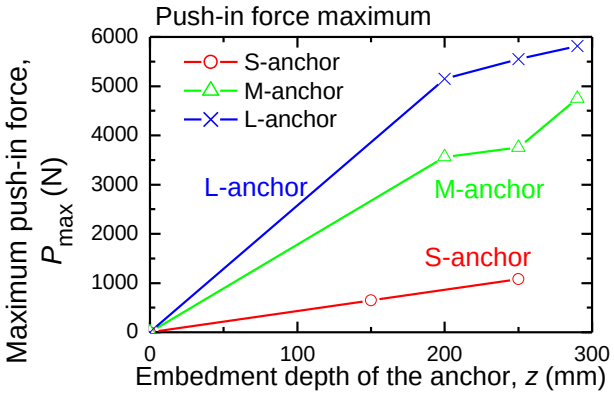

Fig. 8 Relationships between maximum push-in force and embedment depth of the anchors

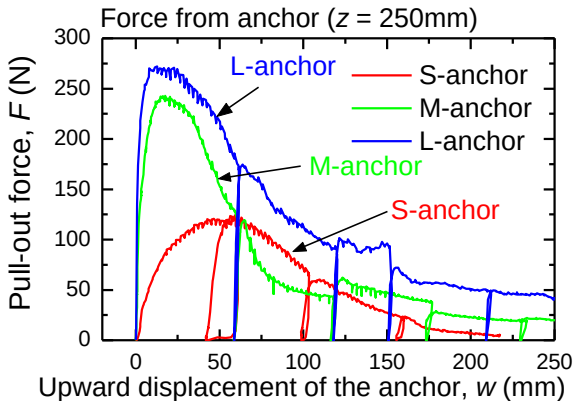

Fig. 9 Relationships between pull-out force and upward displacement of the anchors

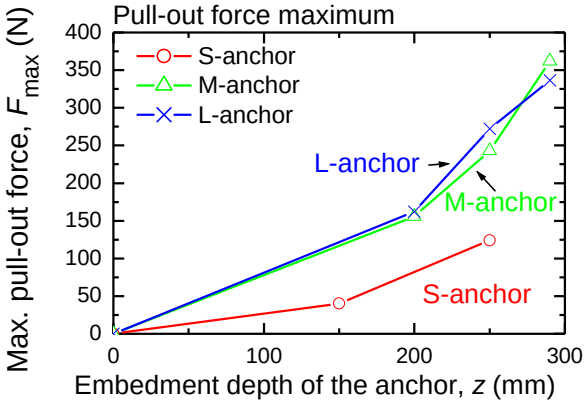

Fig. 10 Relationships between maximum pull-out force and embedment depth of the anchors

It is seen from the comparison of **Fig. 8** and **Fig. 10** that:

(1) the maximum push-in force is much higher than the maximum pull-out force in each anchor

(2) the maximum push-in force increased as the size of the anchor increased (**Fig. 8**)
(3) the maximum pull-out forces of the anchors were comparable in L-anchor and M-anchor (**Fig. 9**).

In the push-in and pull-out tests of anchors mentioned above, it was not clear whether the anchor head opened fully or not during the pull-out process. Hence, the pull-out tests of embedded anchors were carried out as described in the next section.

4. Pull-out experiments

4.1. Outline

To investigate the basic properties of the anchors further, only pull-out experiments of the buried anchors were carried out. The model sand ground and the testing procedure used in the push-in and pull-out experiments described in Section 3 were also employed in the pull-out experiments.

4.2. Experiment procedure

In a pull-out experiment, the anchor was buried in the model ground in the stage of preparation of the model ground, as shown in **Fig. 11**. The anchor was buried in the ground with its anchor head opened or closed as shown in **Fig. 12**. In the case of opened head condition, embedment depth, *z*, of the anchor is the depth of the wing. Meanwhile, in case of closed head condition, *z* is depth of the top end of anchor, because it was thought that the closed anchor turns around the top end of anchor at an initial stage of pull-out process.

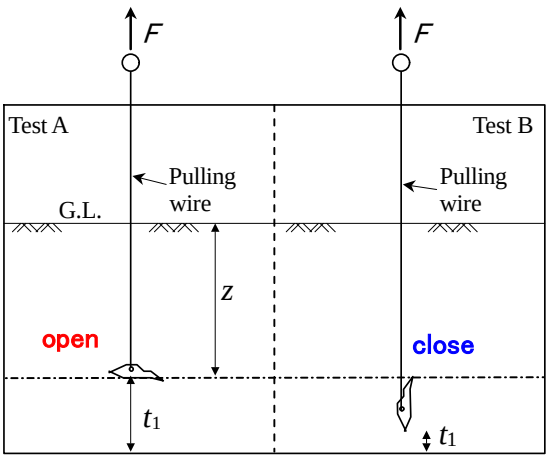

Fig. 11 Outline of pull-out experiment

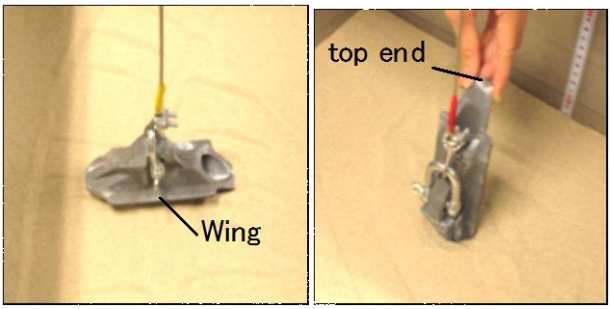

Test A: Opened Test B: Closed

Fig. 12 State of anchor head buried. Open / Close

S-, M- and L-anchors were used again. Embedment depths, *z*, of S-anchor were 150, 250 and 395 mm. In the cases of M-anchor and L-anchor, *z* = 200, 250, 290 mm. That is, a total of 18 pull-out experimental cases, were conducted.

4.3. Experimental results

Figs. 13 to 18 show relationships between pull-out force, *F*, and upward displacement of the anchor, *w*. **Figs. 13, 15** and **17** are the relationships of S-anchor, M-anchor and L-anchor buried with opened head state. **Figs. 14, 16** and **18** are those with closed head state.

In each anchor, the pull-out resistance force, *F*, became larger as embedment depth, *z*, got deeper, regardless of the anchor head state (opened or closed) when buried.

It is seen from comparison of **Fig. 13** (S-anchor, opened) and **Fig. 14** (S-anchor, closed) that the maximum pull-out force, F_{max}, acting on the opened anchor was larger than that on the closed anchor. However, the force acting on the opened anchor decreased immediately after the peak, while the maximum force acting on the closed anchor persisted showing a favourable behaviour. Similar trends were observed in the cases of M- and L-anchors, except that F_{max} of the anchors with the closed head state were larger than those with the opened head state.

Figs. 19 and **20** show the relationships between the maximum pull-out force, F_{max}, and the embedment depth of the anchor, *z*, in the cases of opened head state and closed head state, respectively. Regardless of the setting condition of the anchor heads, the maximum pull-out force, F_{max}, increased exponentially as the embedment depth, *z*, increased. That is, the increasing rate of F_{max} against *z* became larger as *z* became larger.

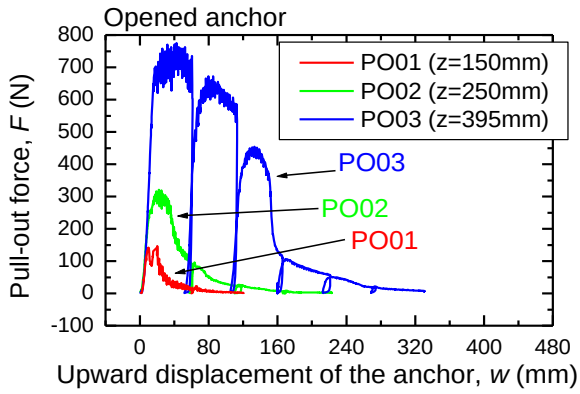

Fig. 13 Relationship between pull-out force and upward displacement of opened S-anchor

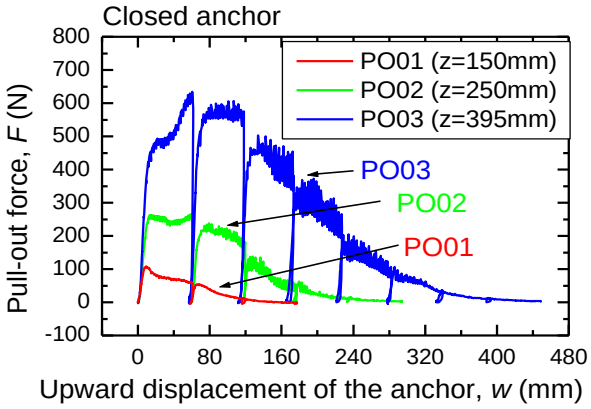

Fig. 14 Relationship between pull-out force and upward displacement of closed S-anchor

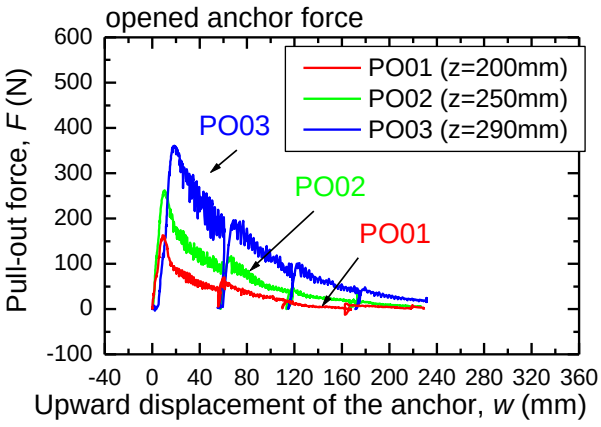

Fig. 15 Relationship between pull-out force and upward displacement of opened M-anchor

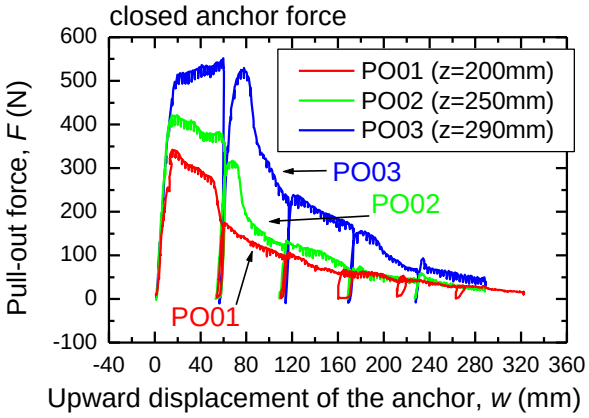

Fig. 16 Relationship between pull-out force and upward displacement of closed M-anchor

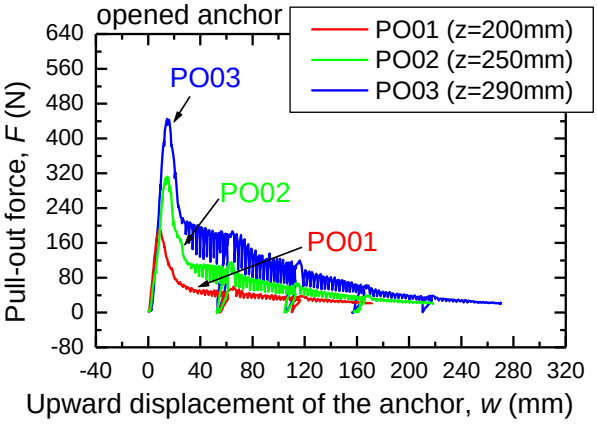

Fig. 17 Relationship between pull-out force and upward displacement of opened L-anchor

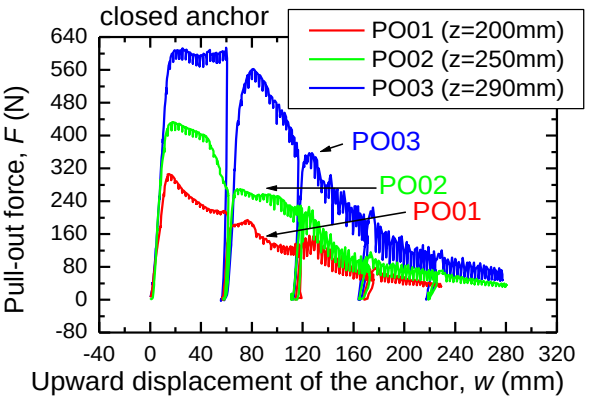

Fig. 18 Relationship between pull-out force and upward displacement of closed L-anchor

The authors expected smaller F_{max} for the anchors with the closed head state, but the experimental results were contrary to our expectation in the cases of M- and L-anchors. One of reasons for this may be attributed to rotational resistance of the closed anchor when it is pulled-out. It is difficult, however, to derive a definite reason for this aspect at present. Hence, the experimental results of the anchors with opened head state are discussed in detail hereafter.

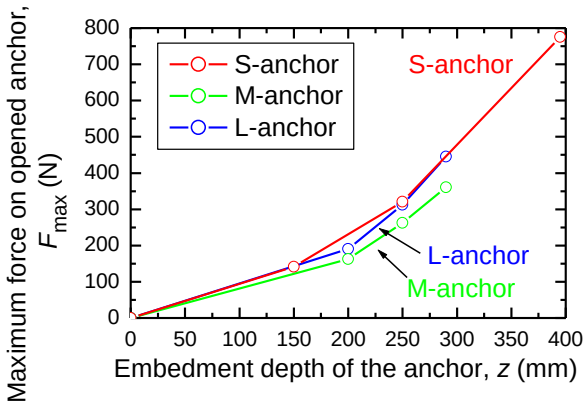

Fig. 19 Relationship between maximum pull-out force on opened anchor and embedment depth of opened anchor

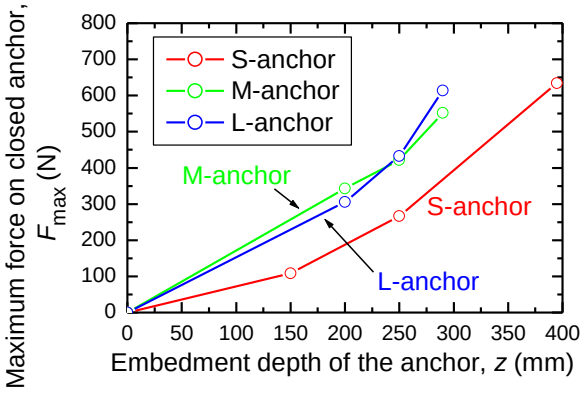

Fig. 20 Relationship between maximum pull-out force on closed anchor and embedment depth of closed anchor

Fig. 21 shows the relationship between the maximum stress acting on the opened anchor, p_{max} (= F_{max}/A), and the embedment depth, z. As the anchor projected area, A, decreased, the maximum pull-out stress increased. If the maximum pull-out stress, p_{max}, depends only on the overburden pressure acting on the anchor area, p_{max}, should be only 0.005 N/ mm^2 when the embedment depth z is 300 mm, for example. However p_{max} on M-anchor and L-anchor reached about 10 times of this value and that on S-anchor reached 50 times value of it.

Fig. 22 shows the state of ground surface after pulling out M-anchor (z = 290mm). The heaving area of the ground surface was larger than projected area of the anchor. This tendency was more conspicuous as z was larger. In order to investigate the mechanism of pull-out resistance of the opened head anchors in detail, push-up experiments of a trap door simulating an anchor was conducted.

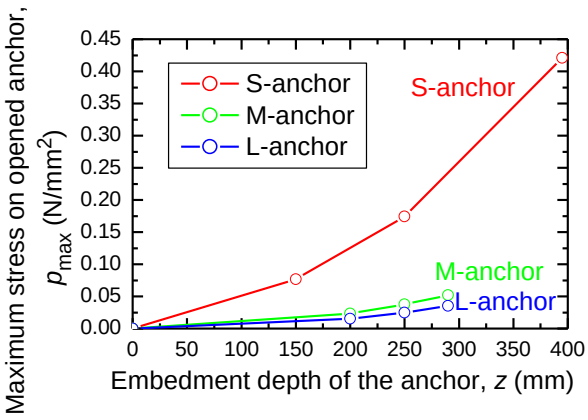

Fig. 21 Relationship between maximum pull-out stress and embedment depth of opened anchor

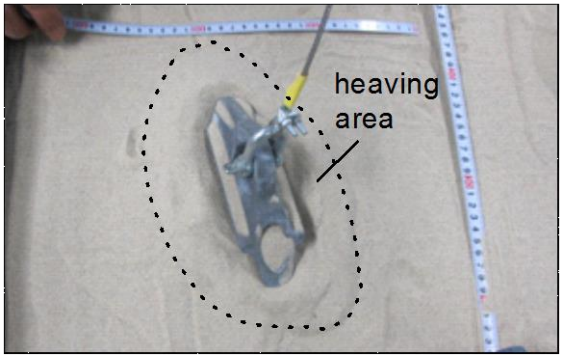

Fig. 22 State of ground surface after pulling out an anchor

5. Push-up experiments of a trap door simulating an anchor

5.1. Outline of experiments

An experimental setup shown in **Fig. 23** was used in push-up experiments of an anchor (trap door). A sand box (width 800 mm, height 500 mm, depth 98 mm) is made of transparent acrylic plates. A trapdoor (width 80 mm, made of Teflon) is set up on the bottom of the sand box. The trapdoor can be lifted up by 50 mm by means of a loading jack. Thus, push-up experiments of the trapdoor were carried out simulating an anchor.

Push-up force, F, and push-up displacement, w, were measured by a load cell and a dial gauge respectively. The anchor was pushed-up at a rate of about 0.1 mm/s. Sampling frequency of the data was 2 Hz.

The model ground was made from dry silica sand #3. The physical and mechanical properties of the silica sand are listed in **Table 2.** The internal friction angles at peak strength and at residual strength, ϕ_p' and ϕ_r', were obtained from a triaxial consolidated drained shear test of the sand with a confining pressure, p_0, of 11 kPa. Friction

angle between the trapdoor and the silica sand was obtained from a direct shear test between them and estimated as 20 degrees.

The model ground was prepared by about 50 mm layers. At first, the silica sand of about 50 mm height was put in the sand box. Next, the sand layer was tapped to adjust the sand to a predetermined dry density of ρ_d = 1.512 g/cm^3 (relative density D_r = 80%).

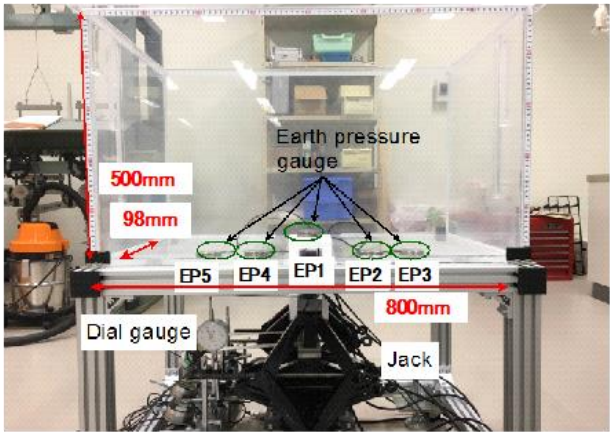

Fig. 23 Photo of anchor push-up experiment setup

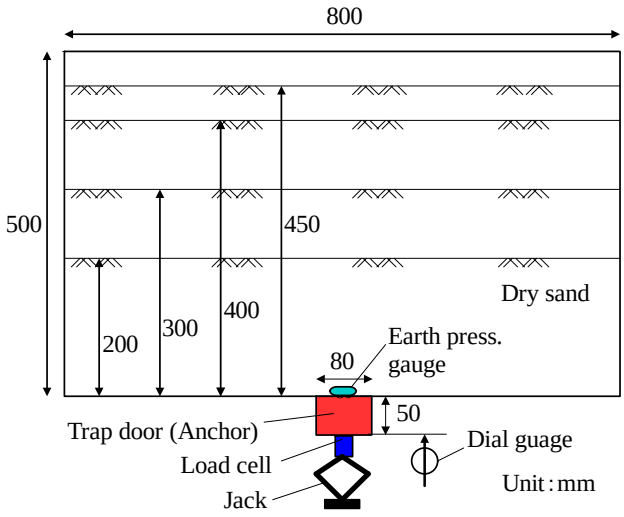

Fig. 24 Anchor push-up experiment setup

Table 2. Physical and mechanical properties of the silica sand

Density of soil particles, ρ_s (g/cm^3)	2.632
Max.dry density, ρ_{dmax} (g/cm^3)	1.567
Min.dry density, ρ_{dmin} (g/cm^3)	1.325
Max. void ratio, e_{max}	0.987
Min. void ratio, e_{min}	0.679
Int. friction angle at peak strength, ϕ_p' (deg)	39.6
Int. friction angle at residual strength, ϕ_r' (deg)	36.6

A total of four experiments were carried out with different h of 200, 300, 400 and 450 mm (**Fig. 24**). **Fig. 25** is an example of model ground having a height, h, of 200 mm.

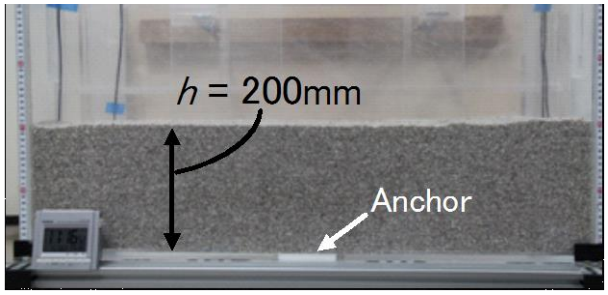

Fig. 25 Sample of model ground

5.2. Image analysis of the ground deformation

The deformation of the model ground during the push-up experiment was monitored using an image analysis, taking an advantage of the transparent soil box.

A camera was set in front of the sand box. Photographing interval was 2 seconds. The photos taken during the experiment were processed by using the image analysis software "Trackpy".

5.4. Experiment results

Fig. 26 shows the relationship between push-up force, F, acting on the anchor and upward displacement of the anchor, w. The push-up force, F, increased as the height of ground above the anchor. It is interesting that w at the peak of F increased as h increased.

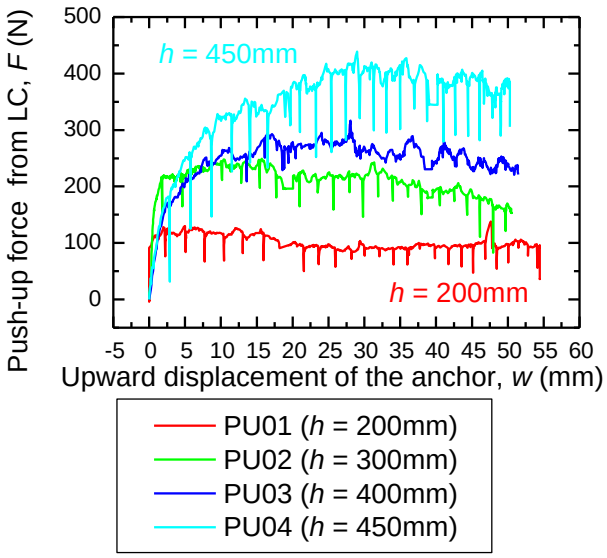

Fig. 26 Relationship between push-up force acting on the anchor and upward displacement of the anchor

Fig. 27 shows the relationship between the maximum push-up force, F_{max}, and the height of the ground, h. It is seen from the figure that F_{max} increased exponentially with increasing h.

The calculated results will be explained and discussed in Section 5.5.

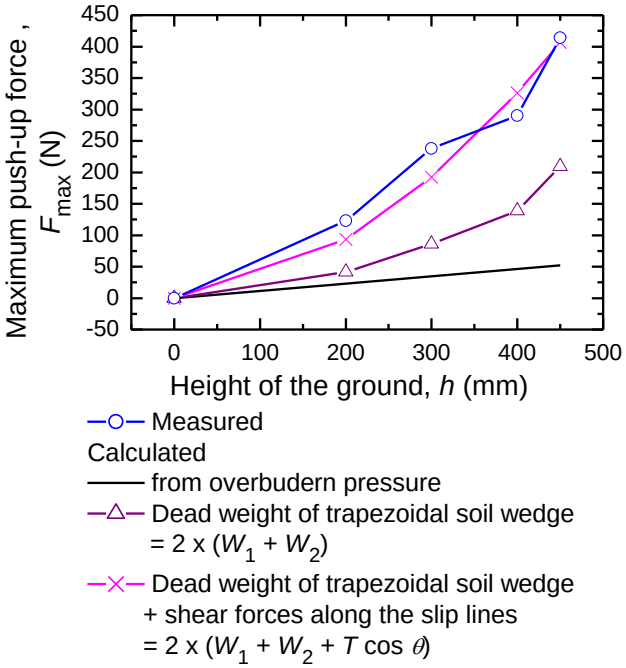

Fig. 27 Relationship between the maximum push-up force F_{max} and height of the ground h

5.5. Modelling of ground failure

A failure pattern of the ground was modelled simply from the ground behaviour obtained by the image analysis. Based on that, a relationship between the maximum push-up force, F_{max}, and the ground height, h, is discussed.

Fig. 28 shows the traces of the soil particles (coloured lines) obtained in all the experiments until the anchor (trap door) was push-up to 50 mm. The slip lines were identified visually, so that clear distinct of movements of the soil particles can be found. Large amounts of the movements of the soil particles are detected inside the slip lines, while almost no movements of the soil particles are found outside the slip lines.

Straight slip lines are generated from both ends of the anchor, the angles between the slip lines from the vertical direction are 20 degrees in all the cases regardless of height of the ground.

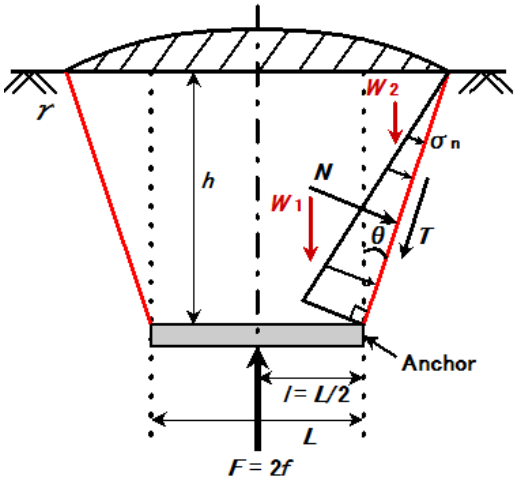

Fig. 29 Modelling of ground failure

Fig. 29 is a simple model of ground failure mechanism. The symbols shown in **Fig. 29** are as follows:

h: embedment depth of anchor

γ: unit weight of soil

W_1: $W_1 = \gamma \times l \times h \times D$ (D: depth of anchor)

W_2: $W_2 = (1/2) \times \gamma \times h \times h\tan\theta \times D$

θ: angle of slip line

N: normal force acting on slip line

T: shear force acting along slip line, $T = N\tan\phi'$

L: width of anchor

l: $l = L/2$

f: force acting on the half of anchor

$f = W_1 + W_2 + T\cos\theta$

F: total force acting on anchor, $F = 2 \times f$

σ_n: $(1+K_0)\sigma_v/2 + (1-K_0)(\sigma_v/2)\cos\theta$

(σ_v: Effective earth pressure,

K_0: coefficient of earth pressure at rest)

In this experiment, K_0 was supposed to be 1 because the model ground was compacted by tapping.

θ may correspond to the influential angle, β, specified in the *Standards for Design and Construction of Ground Anchors and Commentary* (JGS, 2012). β is specified as $\beta = (2/3)\phi$, where ϕ is the internal friction angle of the soil. If ϕ is assumed to be equal to ϕ_r' or ϕ_p' (refer to **Table 2**), β ranges from 24.4 to 26.4 degrees. This range is larger than the measured θ of 20 degrees.

In **Fig. 27**, the relationships between the calculated maximum push-up force acting on the anchor, F_{max}, and the ground height, h, are shown together with the measured result (○ marks). Three types of the

calculations were conducted. The black line (−) is the dead weight of the rectangular soil only above the anchor (= $2\times W_1$). The triangle mark (△) is the dead weight of the inverse trapezoidal soil wedge above the anchor [= $2\times(W_1+W_2)$]. The cross mark (×) is the sum of the dead weight of the inverse trapezoidal soil wedge above the anchor and the vertical components of the shear forces along the slip lines [= $2\times(W_1+W_2+T\cos\theta)$].

It is seen from **Fig. 27** that the theoretical values (×) agree with the experimental values (○) qualitatively and quantitatively.

Similar patterns of the ground failure seems to occur in three dimensional conditions, as the heaving area at the ground surface observed in the pull-out experiment of an anchor was larger than the project area of the anchor, as has been shown in **Fig. 22**.

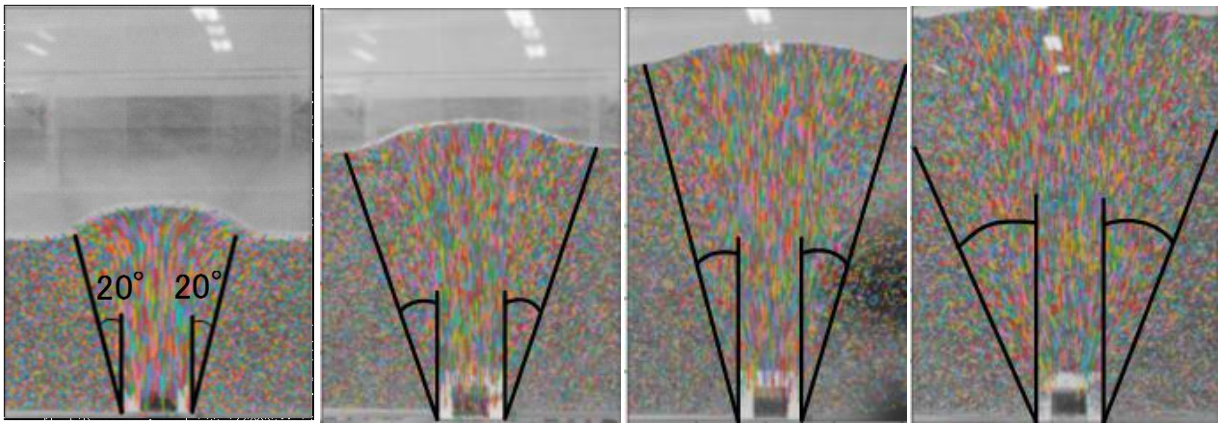

(a) h = 200 mm (b) h = 300 mm (c) h = 400 mm (d) h = 450 mm

Fig. 28 Behaviour of sand and slip line by image analysis

6. Concluding remarks

In order to investigate fundamental pull-out resistance mechanisms of flip-type anchors, a series of push-in and pull-out experiments, and pull-out experiments of the anchors in a dry sand model ground were carried out. In the pull-in and pull-out experiments, the anchors with different sizes were pushed into the model ground and then were pulled out.

In the pull-out experiments, the anchors were buried in the model ground with its head opened or closed. The pull-out resistance of anchors with closed head state was larger than those with opened head state, contrary to the authors' expectation. Although a reason for this result may be attributed to rotational resistance of the closed anchor when it is pulled-out, further investigation is needed for this aspect.

Furthermore, push-up experiments of a trap door simulating an anchor were carried out, in order to investigate mechanisms of the pull-out resistance of anchors in more simplified experimental conditions (plane strain conditions). An image analysis of the ground deformation was employed in the push-up experiments. Based on the image analysis, ground failure pattern was simply modelled, in which an inverse trapezoidal soil wedge on the anchor was pushed up. The calculated values of the maximum push-up forces of the anchor (trap door) based on the ground failure model were in good agreement with the measured results. Similar patterns of the ground failure also seems to occur in three dimensional conditions.

The authors are aware that the push-up experiments in this paper do not perfectly reproduce behaviours of the ground of an actual anchor, in which soil particles move into a cavity created under the anchor.

Further experiments including vertical pull-out experiments using flip-type model anchors, diagonal pull-out experiments of the anchors, and pull-out experiments of the anchors in slopes in two and three dimensional conditions are planned to be conducted in our future research.

Reference

Anchoring Rope and Rigging Pty Ltd. 2018. Hulk Earth Anchors, http://www.hulkearthanchors.com/.

Japanese Geotechnical Society. 2012. Standards for design and construction of ground anchors and commentary. JGS 4101-2012. (in Japanese)